Rate theory cluster dynamics simulations including spatial correlations within displacement cascades

T. Jourdan* and J.-P. Crocombette
CEA, DEN, Service de Recherches de Métallurgie Physique, F-91191 Gif-sur-Yvette, France
(Received 16 May 2012; revised manuscript received 18 July 2012; published 20 August 2012)

Mean-field cluster dynamics (CD) using rate theory is a convenient method to simulate the nucleation, growth, and coarsening of clusters under continuous irradiation or ion implantation up to high doses. When displacement cascades are produced, clusters are directly nucleated in cascades, so that creation rates of clusters must be introduced in CD. However, these rates are difficult to determine since CD cannot intrinsically account for spatial correlations between clusters in cascades. In this article a space homogenization method is proposed to determine an effective irradiation source term for CD, based on the knowledge of the primary damage and on a modified kinetic Monte Carlo algorithm. The effective irradiation term is shown to be dynamic, in the sense that it depends on the cluster density in CD simulations. The interest of the method is demonstrated in iron in the case of 20-keV primary knock-on atoms and 60-keV helium implantation.

DOI: 10.1103/PhysRevB.86.054113 PACS number(s): 61.72.Cc, 82.20.Wt, 61.72.J−, 66.30.Lw

I. INTRODUCTION

Irradiation of materials with ions and neutrons, as well as ion implantation, lead to displacement cascades, which are locally damaged regions where point defects [vacancies and self-interstitials atoms (SIAs)] and point-defect clusters are generated. The formation of such localized damage, with a significant fraction of defects produced in clusters, highly affects the long-term microstructural evolution and has a direct influence on the macroscopic properties of materials. In general, two steps can be identified in the formation of defect clusters in cascades.[1] First, clusters can be created during the initial development of the cascade, in either the ballistic phase or the thermal spike.[2,3] This phase, which lasts a few tenths of a picosecond over a few tens or hundreds of nanometers, can be modeled by molecular dynamics (MD) simulations or by its binary collision approximation (BCA). Second, migrating species inside the cascade region can interact with other clusters in the same cascade or leave the cascade region and interact with other elements of the microstructure, such as debris from other cascades, dislocations, and grain boundaries.[4] This second step, which is linked to the long-range diffusion of defects, spans length scales from a few nanometers to a few microns, typical of a grain size, and time scales from nanoseconds to years.

To simulate such large systems over long times, object kinetic Monte Carlo (OKMC)[4,5] or event-based kinetic Monte Carlo (EKMC)[6,7] methods are often used. In this type of approach, referred to hereafter as the kinetic Monte Carlo (KMC), each cluster is considered as a single object that can migrate, absorb, and emit other species. Since the position of objects is considered, this method naturally accounts for spatial correlations between clusters within cascades. However, a major limitation of KMC is the difficulty to reach irradiation doses higher than about 0.1 displacement per atom (dpa), due to the computational burden of such calculations.

To circumvent this problem, mean-field rate theory, also called cluster dynamics (CD), has to be used.[8] This approach is similar to KMC, insofar as the migration, reaction, and dissociation of clusters are considered. However, only cluster concentrations are retained, so that a set of ordinary differential equations is solved to determine the concentrations as a function of time. In such reaction rate equations, irradiation is introduced as a creation rate term for some cluster types. CD is of common use in metals under various irradiation conditions (e.g., Refs. 8 and 9) and is also used in semiconductors after ion implantation.[10,11]

KMC and CD simulations can be compared at any physical time on the basis of cluster distributions. Without irradiation, it has been shown that a very good agreement is obtained for the homogeneous precipitation under thermal aging[12] and the annealing of self-defects.[13] Under irradiation, the agreement is also very good provided that spatial correlations between defects created in KMC are artificially suppressed.[14,15] When spatial correlations are considered in KMC, which is the case when cascades provided by MD or BCA calculations are directly introduced in the simulation, severe discrepancies generally exist between CD and KMC results.[15–17] Such differences arise because CD, due to its mean-field formalism, can only consider the creation of defects without spatial correlations. To circumvent this difficulty it is customary to consider the creation rates of clusters in CD as parameters which are fitted to reproduce cluster distributions obtained by KMC or experimental measurements.[9] This approach raises the question of the predictability of CD calculations, given the large influence of creation rates on the nucleation of clusters and the number of possible fitting parameters: one has to choose the type of clusters which are created under irradiation and the associated creation rate.

Attempts to design an accurate source term for CD are based on the annealing of isolated cascades with KMC for a sufficient time, in order to suppress spatial correlations. Concentrations of remaining defects at the end of annealing can then be used to build an effective source term. This method, however, raises the fundamental question of the choice of the annealing time. For example, in α-iron first-principle calculations have shown that SIA migration energy is 0.34 eV, whereas vacancy migration occurs with a migration energy equal to 0.67 eV.[18] Assuming as a first approximation the same diffusion prefactor for these two defects, at room temperature

 ©2012 American Physical Society

the ratio of diffusion coefficients is around 3.10^5. As already pointed out in Refs 19 and 20, SIAs will therefore homogenize more quickly than vacancies. Such differences in diffusion coefficients are very common, so this problem appears in a large number of metals, semiconductors and insulators. To our knowledge, a parameter-free and physically motivated method to build a source term for CD is still lacking.

In the present paper we propose a simple yet powerful method to address with CD the multitime and multiscale process corresponding to the migration and clustering of defects within and between cascade regions. We show that, in general, no annealing time can be defined in the KMC to provide a correct source term for CD, but an easy-to-implement modification can be made in KMC to build a space homogenization procedure. This procedure provides a source term for CD which correctly reproduces cluster distributions obtained in KMC simulations. Effectiveness and accuracy of the method are shown for 20-keV cascades in α-iron and helium implantation at 60-keV in α iron. The first example is a test of the method for rather large cascades or subcascades, whereas the second example shows a case of a spatially dependent source term representative of light ion implantation.

II. SIMULATION METHODOLOGY

As explained above, to simulate the evolution of clusters under cascade production conditions, at least two methods must be coupled. The first one provides primary damage in terms of the position of defects inside a cascade and is used to build a cascade database. The second is a kinetic simulation to calculate the evolution of clusters due to their migration, reaction with other clusters, and dissociation.

Our goal is to build a correct source term for CD kinetic simulations. We therefore need a reference kinetic simulation to check the CD simulations. This reference is provided by a complete KMC run in which cascades are introduced one after the other and evolved over long times. Note that such a brute force approach requires very large computation times and can only be used to produce reference results for selected test cases.

The results of the full KMC simulations will be compared with mean-field CD with various source terms. Three types of source terms will be considered, resulting from raw cascades (no annealing), standard constant-time annealing within the KMC of single cascades, and our sphere homogenization procedure. In Sec. II A we briefly describe the tools we have used for primary damage, KMC, and CD simulations. In Sec. II B, we describe our sphere homogenization procedure and the associated modifications of KMC simulations.

A. Simulation techniques

Correlated primary damage was produced by the MARLOWE code.[21] Though less precise than MD simulations, this code enables one to quickly simulate primary damage and have access to the spatial distribution of defects in cascades, which is needed for KMC simulations. Contrary to MD, only point defects are created during cascade development, so clusters will result from the defect migration treated in KMC and CD. Since we are only interested in designing a source term that would allow us to reproduce KMC results with CD, using another simulation technique to provide primary damage would not affect the validity of our homogenization method.

KMC simulations were performed using the EKMC code JERK.[6,7] Contrary to object kinetic Monte Carlo (OKMC) methods,[4,5] atomic jumps of clusters are not considered: instead clusters migrate through continuous diffusion laws. The total simulation time is divided into macro time steps, during which creation, absorption, and dissociation of clusters are performed. At the end of each time step, defects are moved according to their respective diffusion law. Details about the original implementation are provided in Ref. 7. In this work we used an improved version of JERK, which generally leads to considerable speedups without sacrificing precision. The simulation volume is divided into rectangular cells which contain at most a given fixed number of defects. As in the cell method,[22] the interaction list of a defect in a given cell during a macro time step is built by considering all defects in the cell and in neighbor cells, thereby avoiding a full calculation over all defect pairs. The value of the macro time step is chosen so that the mean-square displacement of the fastest defect present in the simulation volume is lower than the smallest cell dimension, so that interactions beyond neighbor cells can be safely neglected. This adaptive time-step scheme has profound implications on the efficiency of the annealing procedure presented in the next subsection.

Finally, CD simulations were done using the CRESCENDO code.[13] It relies on the same input parameters as KMC: diffusion coefficients of objects, binding energies, and reaction distances between interacting objects. Clusters are identified by their number of vacancies or SIAs n and, if needed, their number of solute or gas atoms p. Evolution equations concerning cluster concentrations $C_{(n,p)}$ are presented in Ref. 13. CRESCENDO, as regular CD codes, deals with fully homogenized concentrations. It can also consider a spatial dependence of the equations: the system under study can be divided into slices in one direction and a homogeneous CD is performed in each slice. Slices are coupled to adjacent slices through a Fick's law on mobile species. This version of the code will be used to simulate the highly inhomogeneous damage profile induced by helium implantation.

B. Sphere homogenization method

For the sake of simplicity, we explain in the following how to define an effective source term for homogeneous CD, based on cascades generated by BCA or MD. We call this procedure the sphere homogenization method (SHM). Spatial dependence is treated at the end of this section. We use the term "cluster" for both single defects and defect clusters.

First, N_c cascades are generated to be used as a cascade database. These cascades are then homogenized one by one and a histogram of cluster types is built during this process. To homogenize a cascade, we use a modified KMC code. The KMC being stochastic in nature, for each cascade many different evolutions are possible. We therefore perform N_r KMC runs to sample the various possible evolutions of every cascade. During each run the following steps are performed.

(1) At $t = 0$, insert the cascade in a KMC simulation box.

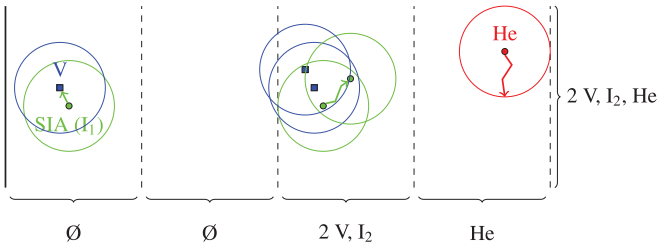

FIG. 1. (Color online) Schematic representation of a typical kinetic evolution in a homogenization simulation by SHKMC. In this example, damage is created by the implantation of a helium atom from the left of the system. The contribution to the effective CD source term is shown at the right for homogeneous CD simulations. When spatial dependency of rate equations is considered, the source term is defined for each slice and is shown here below the braces. Vacancies, SIA clusters containing n SIA, and helium atoms are symbolized by V, I_n, and He, respectively.

(2) Draw spheres centered on the initial position of clusters in the cascade. Each sphere has the same radius r_d, whatever the cluster type.

(3) Proceed to the kinetic evolution of the system with KMC. Once a cluster crosses its sphere, it is suppressed from the simulation box and a contribution of this cluster to the histogram of cluster types is added. If a new cluster is created, a sphere centered on the position of this cluster is drawn. We call this modified version of KMC the sphere homogenization KMC (SHKMC) (Fig. 1).

(4) At $t = t_h$ (final homogenization time), stop the simulation and add the remaining clusters to the histogram of cluster types. Suppress the content of the simulation box and go to step 1.

Once all cascades have been homogenized, the histogram of cluster types is transformed into creation rates of clusters and used as an effective source term in CD. The method is based on two parameters, the sphere radius r_d and the homogenization time t_h. These parameters are not fitted on experiments or KMC results but are determined as follows. In CD, since clusters are homogeneously distributed in space, at any time in a simulation the volume ascribed to a cluster is

$$V_c = \frac{1}{\sum_{n,p} C_{(n,p)}}, \tag{1}$$

where the sum runs over all possible cluster types. The half-distance between first neighbors, assuming a simple cubic arrangement of clusters, is therefore

$$r_c = \frac{1}{2}\left(\frac{1}{\sum_{n,p} C_{(n,p)}}\right)^{1/3}. \tag{2}$$

The sphere radius r_d must be chosen equal to r_c, which appears to be a typical homogenization distance. If r_d is chosen larger than r_c, our modeling setup for homogenization, which consists in a single isolated cascade in the simulation box, is not valid anymore in general. Indeed, if a cluster from the cascade is allowed to migrate over distances larger than r_c during the homogenization process, the probability that a reaction occurs between this cluster and a cluster which is not part of the cascade cannot be neglected. As we do not consider such intercascade clustering in the homogenization procedure, for $r_d > r_c$ intracascade clustering is artificially enhanced. Conversely, if r_d is much lower than r_c, clusters are not allowed to migrate over intermediate distances, which are still lower than the typical distance between clusters in CD, so the homogenization is not complete.

Since the total density of clusters is not constant as a function of time, r_c varies during a CD simulation. Therefore, at any time step in the CD simulation, the source term must be updated with the result of a homogenization performed with $r_d = r_c$. In practice, to determine this dynamic source term, several KMC homogenizations of the cascade database must be performed before a CD simulation with different values of r_d which encompass the values of r_c needed in CD. The precise source term required by CD for any value of r_c can then be determined by interpolating the effective source terms obtained by homogenization for several values of r_d. We show in the next section that using a constant r_d can lead to significant deviations from a reference calculation when the variation of the cluster density is large.

The value of the homogenization time t_h is less constrained than r_d. Increasing the homogenization time leads to a better homogenization of slow clusters, while fast clusters are quickly removed from the SHKMC simulation once they touch their sphere, so in general, t_h should be large enough to enable all clusters to homogenize.

For a spatially dependent CD source term, when a cluster leaves the SHKMC simulation (steps 3 and 4), it is placed at its original position, as determined by the center of its sphere, instead of its final position. Indeed, since the initial and final positions can be in different slices, using the final position would introduce an undesired long-range diffusion effect in the source term. This would overestimate the diffusion of clusters between slices, as it would be partly accounted for in SHKMC simulations and, again, in CD simulations. Another thing to note in spatially dependent CD simulations is that r_d must remain lower than the slice width. In practice, except for the very first simulation stages, i.e., for a very low concentration of clusters, this condition is always respected.

In the next sections we show the effectiveness and accuracy of the sphere homogenization procedure coupled with CD simulations in two cases.

III. 20-KEV CASCADES IN α-IRON

In α-iron, it can be considered that for primary knock-on atoms (PKAs) whose energy is higher than around 20 keV,[23] cascades are split into subcascades. We can thus expect that 20-keV cascades are a representative case of irradiations by neutrons or high-energy ions in terms of spatial correlations. Besides the physical relevance of using 20-keV PKAs, it is known that at this energy the damage is highly correlated,[24] so it is an interesting case to test the validity of the SHM. In the following, doses are expressed in dpa as calculated by the NRT formula,[25] using a displacement threshold energy equal to 40 eV.[26] All calculations are done at 300 K.

The MARLOWE code was used to generate $N_c = 1000$ cascades, which were homogenized with the SHM implemented in JERK during $t_h = 0.1$ s with values of r_d from 10 to 50 a, where a is the lattice parameter of iron. For each radius and each cascade, the number of KMC runs was $N_r = 100$.

The simulation box dimensions were $200a \times 200a \times 200a$ and periodic boundary conditions were used. To provide a reference calculation, full EKMC calculations were performed up to 0.1 dpa with JERK. On average, eight cascades per second were introduced randomly in the box, which corresponds to a damage rate of 10^{-4} dpa s^{-1}. Experimentally, such a high flux is typically obtained with ion irradiations.[27] The combination of the high flux and the high energy of (sub)cascades is aimed to test the SHM under severe irradiation conditions, where its validity could be questioned. Concerning CD simulations with CRESCENDO, no spatial dependence was considered.

For both KMC and CD simulations, a set of physical parameters describing the migration and stability of clusters is needed. As the purpose of the present work is not to develop a new physical model of α-iron under irradiation, we simply used the kinetic and thermodynamic parametrizations described in Ref. 18, which were shown to successfully reproduce the resistivity recovery experiments after electron irradiation at low temperatures. In this model, interstitial clusters containing up to three interstitials and vacancy clusters containing up to four vacancies are mobile.

In Fig. 2 we show the interstitial and vacancy cluster distributions at 10^{-3} dpa obtained by full EKMC simulations and two CD simulations using different source terms. Statistics was improved in full EKMC calculations by running 100 simulations and averaging out cluster concentrations over the runs. In the first CD calculation, the mean number of interstitials and vacancies created in cascades given by MARLOWE was directly used as a source term for CRESCENDO. In the second calculation, the source term was determined by the SHM applied to the MARLOWE cascade database. When no sphere homogenization is performed, cluster distributions completely differ from the reference calculation (EKMC, blue squares), which highlights the importance of spatial correlations on the nucleation and growth of clusters in these conditions. Using the source term given by the SHM leads to results in very good agreement with full EKMC calculations.

To highlight the improvement of the present homogenization procedure over the usual constant-time annealing approaches, annealing simulations of cascades provided by MARLOWE were also performed with standard EKMC, up to various physical times, from $t_a = 10^{-6}$ s to $t_a = 10^{-1}$ s, to determine source terms for CD. Cluster distributions obtained by full EKMC simulations and CD simulations with the different source terms are shown in Fig. 3 at 10^{-3} dpa. The first thing to note is that CD results based on the SHM give the best agreement with full EKMC simulations, compared to CD simulations with a source term obtained by a constant-time annealing method. In addition, when standard annealing is performed in the EKMC, cluster distributions in CD depend greatly on the annealing time. As t_a increases, small mobile interstitial clusters can react with each other during the KMC annealing and the concentration of small

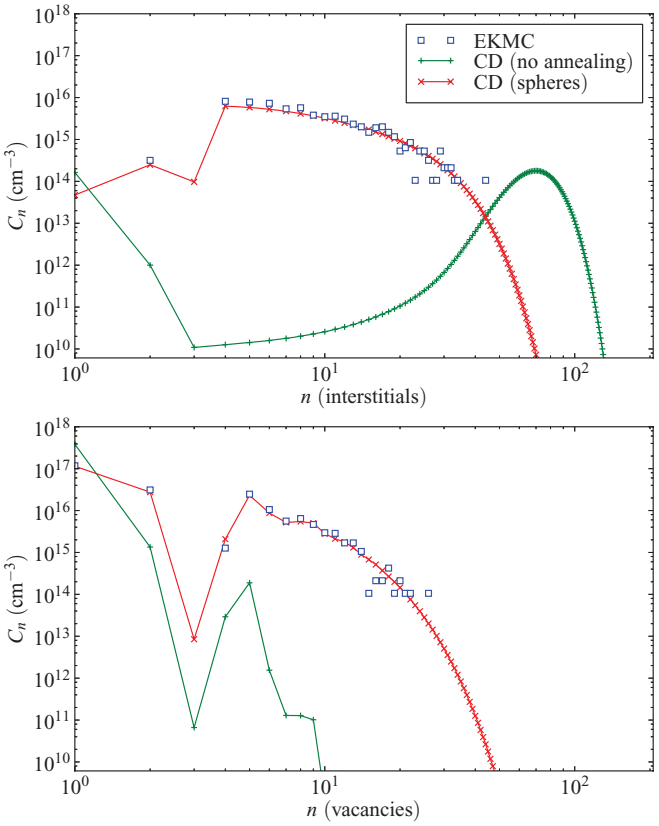

FIG. 2. (Color online) Interstitial and vacancy cluster distributions in iron irradiated up to 10^{-3} dpa at 10^{-4} dpa s^{-1} with 20-keV cascades. Reference calculation is the EKMC simulation. CD calculations were performed without annealing and with the SHM.

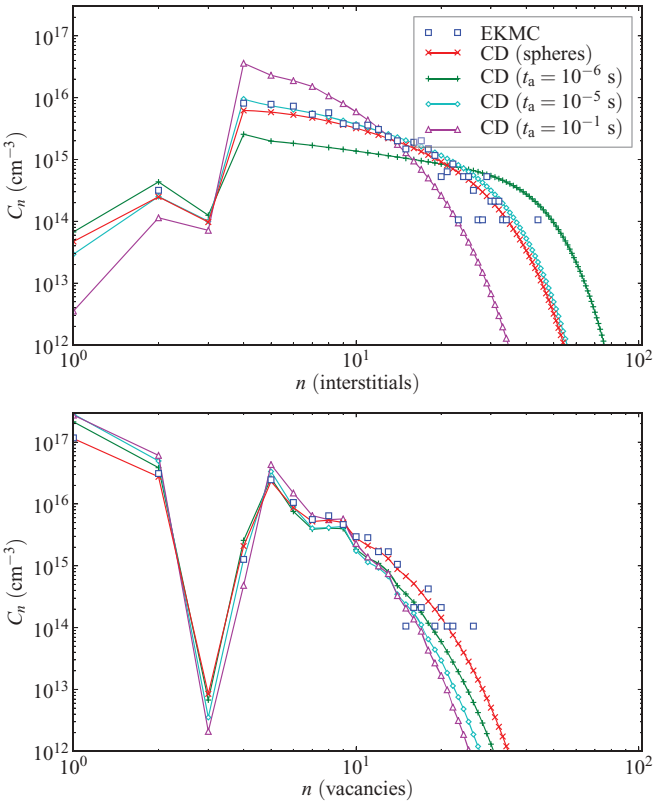

FIG. 3. (Color online) Interstitial and vacancy cluster distributions in iron irradiated up to 10^{-3} dpa at 10^{-4} dpa s^{-1} with 20-keV cascades. Reference calculation is the EKMC simulation. The source term for CD calculations has been obtained either with the SHM or by performing an annealing without spheres, up to various physical times (shown in the legend).

immobile interstitial clusters ($I_{n>3}$) increases. Therefore the source term for these immobile interstitial clusters increases with t_a, while the source term for small mobile interstitial clusters decreases. These two variations result in the formation of a large number of small interstitial clusters in the subsequent CD simulations. As shown in Fig. 3, in order to fit the interstitial distribution obtained in the full EKMC simulations, annealing up to $t_a = 10^{-5}$ s seems an appropriate value. However, in this case the vacancy distribution is not correctly reproduced, especially for the mono- and divacancies, which exhibit higher concentrations when annealing is performed. It can be checked that this discrepancy cannot be solved by increasing the annealing time, so the problem does not come from a too low vacancy clustering rate during annealing. Instead it comes from the fact that during the homogenization process, mobile interstitial clusters quickly reach their spheres and are therefore introduced as such in the source term. In CD they can recombine with vacancies, which lowers V and V_2 concentrations. When spheres are not used, the clustering process of interstitials is not impeded as t_a increases, so the concentration of mobile interstitial clusters decreases during the annealing. The resulting low production term of mobile interstitial clusters in CD is responsible for the high concentration of V and V_2. This point shows that the annealing time is not the appropriate parameter for homogenizing cascades. Conversely, the SHM correctly accounts for the clustering and homogenization of the different defect types, which occur on different time scales depending on their diffusion coefficients.

The relevance of a dynamic source term should also be discussed, since it introduces more complexity in the proposed method. Indeed it must be updated at each time step of CD calculations using the cluster density and preliminary homogenizations with different values of r_d. To investigate this point, a large variation in cluster density is needed and simulations were therefore performed up to 0.1 dpa. In CD calculations, the increase in the cluster density results in a decrease in r_c from $50a$ to $12a$ [Eq. (2)], so r_d should span this range. In this case, due to long simulation times, full EKMC simulations were averaged out over only 30 runs. Results obtained without the dynamic source term are also shown in Fig. 4, using $r_d = 50a$ throughout the CD simulation. It can be seen that when the source term varies as a function of cluster density, the overall agreement with full EKMC calculations is significantly improved. The improvement is particularly noticeable for interstitial clusters, which can be explained as follows. When $r_d = 50a$ is used in the SHM, clusters are allowed to migrate over distances which are larger than r_c in the CD simulation at high doses. During the homogenization procedure, some reactions occur between clusters separated by more than $2r_c$ and less than $2r_d$. The rate of such intracascade reactions is generally too high with respect to what would occur in a full EKMC at a high dose, because intercascade clustering is not considered during the homogenization procedure. This artificial enhancement of the intracascade clustering and thus of the production rate of immobile interstitial clusters is responsible for the higher density of small immobile interstitial clusters in CD, at the expense of large interstitial clusters. Some discrepancies remain for mono- and divacancies and for the distribution tails. Two possible sources of error can

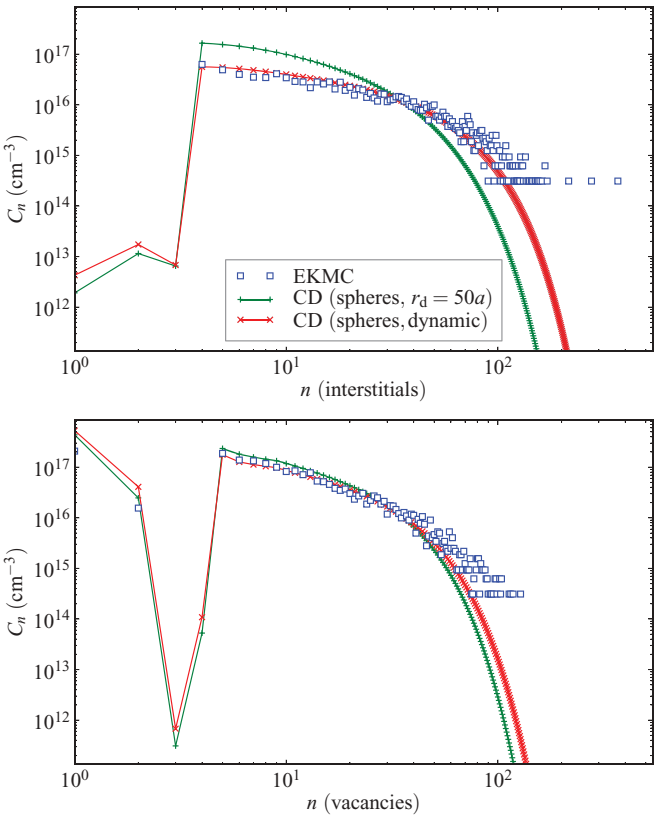

FIG. 4. (Color online) Interstitial and vacancy cluster distributions in iron irradiated up to 10^{-1} dpa at 10^{-4} dpa s^{-1} with 20-keV cascades. The reference calculation is the EKMC simulation. The SHM was used to determine the CD source term. In the first CD calculation, the source term is constant throughout the simulation and corresponds to a homogenization with $r_d = 50a$. In the second calculation, the source term varies with time as a function of the cluster density and corresponds to r_d values between $12a$ and $50a$.

be identified to explain these deviations from the reference EKMC calculations. The first one is independent of the source term. When the cluster density becomes high, the assumptions of CD which are valid in the dilute limit[28] eventually break down.[12] The clustering rate in EKMC is then higher than in CD and the EKMC distribution often exhibits higher concentrations than CD ones for large clusters, as observed in the distribution in Fig. 4. Expressions aimed to improve the validity of CD when the concentration of clusters is high should be used in this case.[29–31] The second source of error is related to the cascade overlap: at such a dose, the probability that a cascade overlaps defect clusters created in previous cascades may not be negligible.[32]

The use of a dynamic source term requires the homogenization of a large number of cascades for different values of r_d. It is thus legitimate to wonder about the computational burden of such calculations and to check that they do not make the method impractical. The computation time needed for the annealing and for the homogenization of 20-keV cascades is plotted in Fig. 5 as a function of KMC time. In the case of the SHM, we consider two different sphere radii corresponding to the lower and upper bounds considered in this section, $r_d = 10a$ and $r_d = 50a$. For small KMC times,

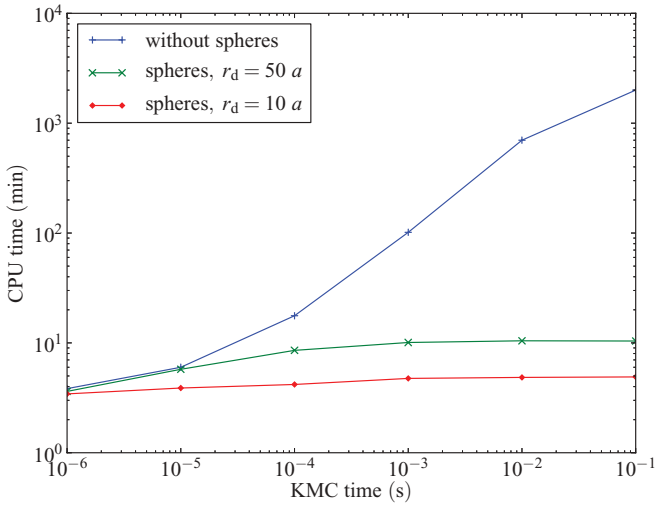

FIG. 5. (Color online) Computation time to anneal or homogenize 10^5 cascades in iron created by a 20-keV PKA, as a function of the KMC time. Homogenization is performed with two values of sphere radii.

nearly no difference exists between the methods. The macro time step in KMC is imposed by the fastest species, which is the monointerstitial. At 300 K, the associated time step is $\Delta t = 5.5 \times 10^{-7}$ s. In the SHM, as time increases, the fastest clusters touch their spheres and are removed from the simulation box. Once only monovacancies and immobile clusters remain in the simulation box, the macro time step becomes equal to $\Delta t = 0.19$ s, so the procedure quickly terminates in at most one macro time step, considering a homogenization time less than or equal to 0.1 s. This is the reason why the computation time reaches a constant value which depends on r_d for the SHM. For the annealing method, fast clusters can remain in the simulation box for a larger time, which considerably slows down the computation.

IV. HELIUM IMPLANTATION IN α-IRON

Helium implantation is the first step in helium desorption experiments,[33,34] whose aim is to probe the stability of small vacancy-helium clusters created during implantation or the subsequent isothermal or isochronal annealings. In this section we consider the implantation of helium in α-iron. In some experiments performed in iron, primary damage is distributed uniformly over the depth[35] and attempts have been made to simulate helium desorption.[36] Others are more difficult to simulate[37,38] because of the highly inhomogeneous implantation and damage profiles. The choice that comes to mind first to simulate implantation in these conditions is KMC, since surfaces can be easily considered and the implantation profile builds up naturally as cascades are introduced in the simulation box. However, helium is highly mobile in α-iron, with a migration energy of around 0.06 eV.[39] This high mobility considerably slows down KMC simulations and makes full KMC modeling of implantation and desorption impossible in practice when helium is implanted at a large fluence. CD does not suffer from this problem, as rate equations are solved deterministically, and it is therefore well adapted provided the effective source term is spatially dependent, in order to capture the effect of the inhomogeneous implantation.

As in the previous section MARLOWE was used to generate $N_c = 10\,000$ cascades created by the implantation of 60-keV helium atoms. At this energy, the ion projected range is 260 nm, i.e., around 900 lattice parameters. Cascades were homogenized during 0.1 s at room temperature in a KMC simulation box whose dimensions were $1000a \times 1000a \times 5000a$, and the number of KMC runs was $N_r = 10$ for each cascade. Periodic boundary conditions were used along the two first directions. In the last direction, boundaries were considered as perfect sinks for all clusters, which means that clusters were removed from the simulation once they reached the surfaces of the sample. The KMC simulation box was subdivided into 100 slices for the SHM, to determine a spatially dependent source term for CD. The same number of slices was used in CD simulations.

Helium flux was equal to 10^{13} He cm^{-2} s^{-1}, which means on average 8237 cascades were introduced in the simulation box per second for full EKMC simulations. The same dimensions and boundary conditions were used as for the SHM. Results obtained by full EKMC simulations were averaged out over 100 runs. The simulations could only be performed up to 0.2 s due to large computation times.

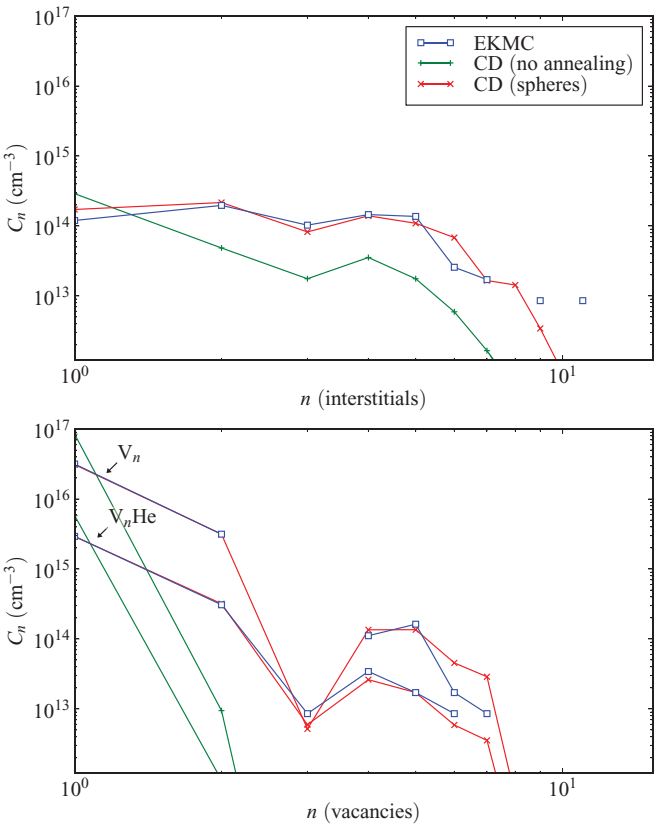

FIG. 6. (Color online) Interstitial and vacancy cluster distributions after implantation of 60-keV helium during 0.2 s with a flux equal to 10^{13} He cm^{-2} s^{-1}. The distribution is shown close to the surface, at depth $z = 14$ nm, only for clusters containing a single helium atom (V_nHe) or no helium (V_n and all interstitial clusters in this case). The reference calculation is the EKMC simulation. CD calculations were performed without annealing and with the SHM.

The parametrization of the model is the same as in the previous section for self-defect clusters. Concerning clusters containing helium, only a single interstitial helium is considered mobile with a pre-exponential factor $D_0/a^2 = 10^{13}$ Hz and a migration energy $E_m = 0.06$ eV. The binding energies of vacancies, SIAs, and helium atoms to vacancy-helium clusters are given by a bubble model parametrized on MD calculations,[40] which is valid over a large range of helium-to-vacancy ratios. This model breaks down for atomic-size clusters and is thus completed by binding energies from density functional theory calculations for clusters containing less than five vacancies.[39] Concerning interstitial loops with helium, we use the linear dependence of the binding energy of a helium atom on the number of interstitial atoms in the loop, obtained by empirical potential calculations.[41] Binding energies of SIAs and helium atoms to helium clusters are taken from density functional theory calculations.[42]

In order to check that the homogenization method is valid in different physical regimes, the comparison between the full EKMC and CD is performed at two depths, $z = 14$ nm and $z = 255$ nm. In the first case, the production rate of self-defects is far higher than the implantation rate of helium. In addition, SIAs and helium atoms quickly migrate to the surface, where they annihilate. We can thus expect the clustering of vacancies to be the main physical phenomenon for the formation of bubbles. In the second case, more deeply in the sample, the helium-to-vacancy ratio is higher. Moreover, interstitials mainly disappear through the recombination with vacancies, so vacancy clusters should be filled with more helium than close to the surface and the growth mechanism can be assisted by the emission of SIAs, if the helium pressure is high enough.[43]

Cluster distributions at these two depths are shown in Figs. 6 and 7 at 0.2 s. Although the physical time is small, the distributions are clearly different, with more pressurized vacancy-helium clusters near the helium implantation peak. In the two cases, CD gives results in close agreement with the full EKMC when the SHM is used. If the production rate of vacancies, SIAs, and helium atoms as obtained by MARLOWE at different depths is directly injected into the spatially dependent CD calculations, cluster distributions are not correctly reproduced. In particular, the vacancy cluster density is systematically underestimated due to the artificial homogenization of primary damage in CD, which reduces the nucleation.

If annealing of cascades is performed instead of the SHM, results are improved with respect to the no-annealing case (Fig. 8). Cluster distributions are shown for an annealing time

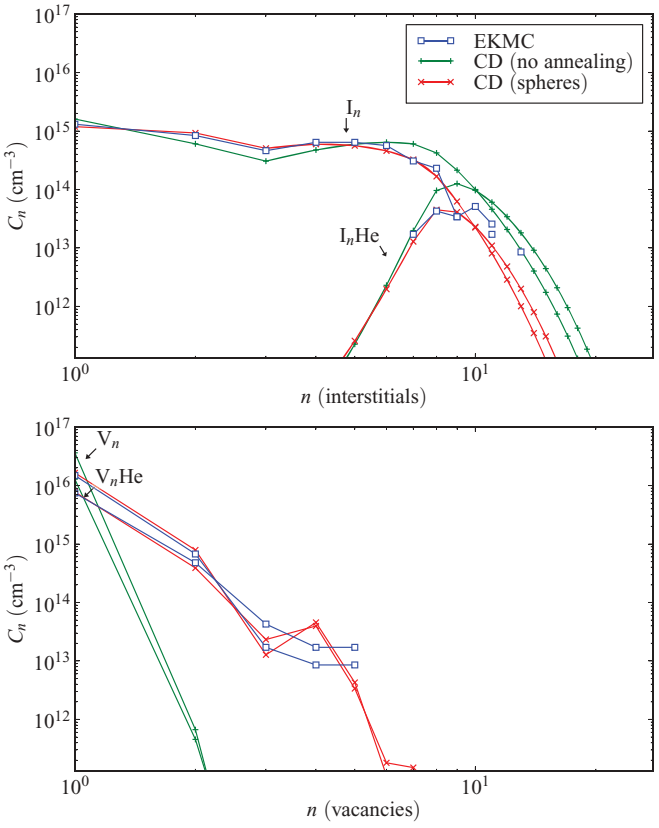

FIG. 7. (Color online) Interstitial and vacancy cluster distributions after implantation of 60-keV helium during 0.2 s with a flux equal to 10^{13} He cm^{-2} s^{-1}. The distribution is shown near the ion projected range, at depth $z = 255$ nm, only for clusters containing a single helium atom (V_nHe, I_nHe) or no helium (V_n and I_n). The reference calculation is the EKMC simulation. CD calculations were performed without annealing and with the SHM.

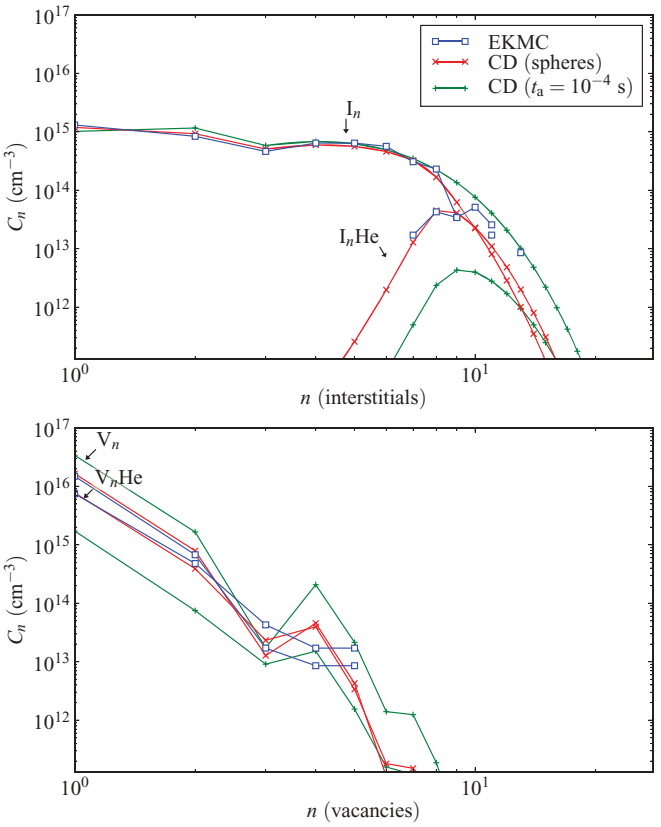

FIG. 8. (Color online) Interstitial and vacancy cluster distributions after implantation of 60-keV helium during 0.2 s with a flux equal to 10^{13} He cm^{-2} s^{-1}. The distribution is shown near the ion projected range, at depth $z = 255$ nm, only for clusters containing a single helium atom (V_nHe, I_nHe) or no helium (V_n and I_n). The reference calculation is the EKMC simulation. CD calculations were performed with a source term given by the SHM or by a standard annealing with $t_a = 10^{-4}$ s.

equal to $t_a = 10^{-4}$ s, which gives the best fit for the interstitial clusters without helium. However, in this case the agreement for the interstitial clusters with helium and the vacancy clusters is rather poor. To explain this discrepancy, it is interesting to estimate the mean-square displacements of some of migrating species during 10^{-4} s. At 300 K, it is $0.2a$ for monovacancies, $108a$ for SIAs, and $(2.4 \times 10^4)a$ for interstitial helium atoms. Interstitial helium thus quickly leaves the cascade region and disappears at the surface during the cascade annealing in EKMC, so the effective source term for interstitial helium is nearly 0. The contributions for clusters containing helium are therefore underestimated by nearly one order of magnitude with the standard annealing procedure. On the contrary, when the SHM is used, interstitial helium quickly reaches its sphere and is included in the effective source term corresponding to the slice where it is implanted. The agreement is good for both vacancy and interstitial cluster distributions, whatever the helium content inside clusters. This emphasizes again the simplicity and the reliability of the method with respect to standard annealing when the number of cluster types with different diffusion coefficients increases.

V. CONCLUSION

In this article we have shown that a specific procedure is needed to transfer the primary damage provided by MD or BCA calculations into mean-field CD calculations. Performing no annealing or an annealing of primary damage during a given time, regardless of the different cluster types, leads to large differences between cluster distributions obtained with CD and with reference KMC calculations.

A method has thus been proposed to account for spatial correlations within displacement cascades in CD simulations. It is based on an intermediate space homogenization step of the primary damage, which produces an effective source term for CD. This SHM can be performed with any OKMC or EKMC code, provided a simple yet crucial modification is done to the standard algorithm, to take account of the different times needed by clusters to homogenize and thus to be treated in a mean-field approach. The procedure is systematic, in the sense that it does not depend on the properties of cascades created by MD or BCA and does not include any fitting procedure.

The method has been tested in iron for cascades created by 20-keV PKA and helium atoms implanted at 60 keV. In both cases, the comparison with KMC simulations showed that the method successfully reproduces cluster distributions, even at doses as high as 0.1 dpa. This procedure must be applied for each set of irradiation conditions (temperature, PKA energy, etc.). Although it cannot be guaranteed always to give results in exact agreement with KMC, its physical justification should make it valid under a large set of conditions.

ACKNOWLEDGMENTS

This work was partially funded by the French National Research Agency (ANR) through Projects HSynThEx (ANR-10-INTB-0905) and CoIrrHeSim (ANR-11-BS09-006).

*Corresponding author: thomas.jourdan@cea.fr

[1] T. Diaz de la Rubia, M. J. Caturla, E. A. Alonso, N. Soneda, and M. D. Johnson, Radiat. Eff. Defects Solids **148**, 95 (1999).
[2] K. Nordlund, M. Ghaly, R. S. Averback, M. Caturla, T. Diaz de la Rubia, and J. Tarus, Phys. Rev. B **57**, 7556 (1998).
[3] D. Bacon, Y. Osetsky, R. Stoller, and R. Voskoboinikov, J. Nucl. Mater. **323**, 152 (2003).
[4] M. J. Caturla, N. Soneda, E. Alonso, B. D. Wirth, T. Diaz de la Rubia, and J. M. Perlado, J. Nucl. Mater. **276**, 13 (2000).
[5] C. Domain, C. S. Becquart, and L. Malerba, J. Nucl. Mater. **335**, 121 (2004).
[6] J. M. Lanore, Radiat. Eff. **22**, 153 (1974).
[7] J. Dalla Torre, J.-L. Bocquet, N. V. Doan, E. Adam, and A. Barbu, Philos. Mag. **85**, 549 (2005).
[8] A. Hardouin-Duparc, C. Moingeon, N. Smetniansky-de-Grande, and A. Barbu, J. Nucl. Mater. **302**, 143 (2002).
[9] E. Meslin, A. Barbu, L. Boulanger, B. Radiguet, P. Pareige, K. Arakawa, and C. C. Fu, J. Nucl. Mater. **382**, 190 (2008).
[10] N. E. B. Cowern, G. Mannino, P. A. Stolk, F. Roozeboom, H. G. A. Huizing, J. G. M. van Berkum, F. Cristiano, A. Claverie, and M. Jaraíz, Phys. Rev. Lett. **82**, 4460 (1999).
[11] C. J. Ortiz, P. Pichler, T. Fühner, F. Cristiano, B. Colombeau, N. E. B. Cowern, and A. Claverie, J. Appl. Phys. **96**, 4866 (2004).
[12] T. Jourdan, J.-L. Bocquet, and F. Soisson, Acta Mater. **58**, 3295 (2010).
[13] T. Jourdan, C. C. Fu, L. Joly, J.-L. Bocquet, M. J. Caturla, and F. Willaime, Phys. Scripta T **145**, 014049 (2011).
[14] J. Rottler, D. J. Srolovitz, and R. Car, Phys. Rev. B **71**, 064109 (2005).
[15] R. Stoller, S. Golubov, C. Domain, and C. Becquart, J. Nucl. Mater. **382**, 77 (2008).
[16] J. Dalla Torre, C.-C. Fu, F. Willaime, A. Barbu, and J.-L. Bocquet, J. Nucl. Mater. **352**, 42 (2006).
[17] C. J. Ortiz and M. J. Caturla, Phys. Rev. B **75**, 184101 (2007).
[18] C.-C. Fu, J. Dalla Torre, F. Willaime, J.-L. Bocquet, and A. Barbu, Nat. Mater. **4**, 68 (2005).
[19] A. Souidi, M. Hou, C. Becquart, L. Malerba, C. Domain, and R. Stoller, J. Nucl. Mater. **419**, 122 (2011).
[20] H. Xu, Y. N. Osetsky, and R. E. Stoller, J. Nucl. Mater. **423**, 102 (2012).
[21] M. T. Robinson, Phys. Rev. B **40**, 10717 (1989).
[22] M. P. Allen and D. J. Tildesley, *Computer Simulation of Liquids* (Oxford University Press, New York, 1987).
[23] S. Jumel and J. C. Van-Duysen, J. Nucl. Mater. **328**, 151 (2004).
[24] R. Stoller, G. Odette, and B. Wirth, J. Nucl. Mater. **251**, 49 (1997).
[25] M. Norgett, M. Robinson, and I. Torrens, Nucl. Eng. Des. **33**, 50 (1975).
[26] *Annual Book of ASTM Standards*, Vol. 2.02 (ASTM International, West Conshohocken, PA, 2004).
[27] F. Fortuna, V. A. Borodin, M.-O. Ruault, E. Oliviero, and M. A. Kirk, Phys. Rev. B **84**, 144118 (2011).
[28] A. D. Brailsford and R. Bullough, J. Nucl. Mater. **44**, 121 (1972).
[29] A. D. Brailsford, R. Bullough, and M. R. Hayns, J. Nucl. Mater. **60**, 246 (1976).

[30]J. Lépinoux, Philos. Mag. **86**, 5053 (2006).
[31]F. Berthier, I. Braems, E. Maras, J. Creuze, and B. Legrand, Acta Mater. **58**, 2387 (2010).
[32]F. Gao, D. Bacon, A. Calder, P. Flewitt, and T. Lewis, J. Nucl. Mater. **230**, 47 (1996).
[33]F. Corni, C. Nobili, G. Ottaviani, R. Tonini, G. Calzolari, G. F. Cerofolini, and G. Queirolo, Phys. Rev. B **56**, 7331 (1997).
[34]G. F. Cerofolini, G. Calzolari, F. Corni, S. Frabboni, C. Nobili, G. Ottaviani, and R. Tonini, Phys. Rev. B **61**, 10183 (2000).
[35]R. Vassen, H. Trinkaus, and P. Jung, Phys. Rev. B **44**, 4206 (1991).
[36]C. J. Ortiz, M. J. Caturla, C. C. Fu, and F. Willaime, Phys. Rev. B **75**, 100102(R) (2007).
[37]R. Sugano, K. Morishita, A. Kimura, H. Iwakiri, and N. Yoshida, J. Nucl. Mater. **329–333**, 942 (2004).
[38]D. Xu and B. D. Wirth, J. Nucl. Mater. **403**, 184 (2010).
[39]C. C. Fu and F. Willaime, Phys. Rev. B **72**, 064117 (2005).
[40]T. Jourdan and J.-P. Crocombette, J. Nucl. Mater. **418**, 98 (2011).
[41]L. Ventelon, B. Wirth, and C. Domain, J. Nucl. Mater. **351**, 119 (2006).
[42]C. C. Fu and F. Willaime, J. Nucl. Mater. **367–370**, 244 (2007).
[43]H. Trinkaus, Radiat. Eff. **78**, 189 (1983).